Mathematical Sciences Letters
An International Journal

http://dx.doi.org/10.18576/msl/090303

Study of Variable Viscosity and Thermal Conductivity of Casson Fluid Flow over a stretching Sheet with Heat Source/Sink Effects

M Nazim Tufail and M Fahad Nadeem

Department of Mathematics, University of Management and Technology, Sialkot, 51310, Pakistan.

Received: 16 Jul. 2020, Revised: 22 Aug. 2020, Accepted: 24 Aug. 2020.
Published online: 1 Sep 2020.

Abstract: In this analysis, the impacts of variable viscosity and thermal conductivity on MHD heat transfer flow of Casson fluid are analyzed on linearly stretching sheet inserted in a porous medium with heat source / sink and viscous dissipation. Then, by using a specific form of Lie group transformations are converted into ordinary differential equations of the governing partial differential equation and Runge-Kutta fourth order strategy is used to numerically solve the differential equations. Numerical results get for various parameters by employing coding in MATLAB programming like viscosity variation A, heat source/sink parameter S, thermal conductivity ε, magnetic field parameter M, permeability parameter k_1, Prandtl number Pr, and Eckert number Ec are investigated. The impacts on velocity and temperature profile of distinct flow parameters are discussed through graphical representation and tables.
Keywords: Variable viscosity; MHD; Stagnation point; Casson fluid; Heat source/sink effects.

1 Introduction

For many production procedures in the sector, like polymer sheet extraction, wiring sketching, paper, glass fiber manufacturing and hot rolling, the stretch sheet flow is a crucial issue in classical fluid mechanics. Many researchers have been worked on stretching sheet but initially Crane [[1]] explored the steady boundary layer flow over a linear stretchable plate accompanied by incompressible viscous fluids provided an precise similarity solution in near to analytical form. Further, C.K. Chen and M. I. Char [2] worked on transferring heat from a constant suction or blowing stretching surface. I. Pop and T.Y. Na [3] analyzed the unsteady flow over a stretchable sheet. K. Vajravelu [4] discussed viscous flow past a nonlinearly stretching sheet. R. Cortell [5] examined the viscous flow and heat transfer above a nonlinearly elastic sheet. L. Zheng, L. Wang and X. Zhang [6] found unsteady boundary layer flow and heat transfer analysis on a permeability stretch sheet with non-uniform heat sources/sinks effects. K. Bhattacharyya [7] inspected the impact of radiation and heat source/sink on unsteady MHD boundary layer flow and heat transfer above a contract sheet along source/sink impacts. M.A.A .Mahmood and S.E. Waheed [8] studied on MHD flow and heat transfer through an extending surface (absorption) and a slip velocity of the micro-polar fluid. Because of the promising implementation of non-Newtonian liquid scientists were interested in further exploring this sort of liquid, one of which was the Casson fluid. Casson fluid is categorized as much admired non-Newtonian fluid, and has many examples in food processing, metallurgy, drilling operations and bio-engineering running. For the forecast of pigment-oil suspensions flow conduct, Casson fluid was launched by Casson in 1959 [9]. According to Dash et al. [10] and Fung [11] the existence of multiple substances, like globulin in aqueous plasma base, fibrinogen and red blood cells can also allow for human blood to be handled as the Casson fluid. Shawky [12] has worked on MHD Casson heat fluid flow over an expanding sheet through a porous medium. Shateyi and Marewo [13] studied on hydromagnetic boundary layer flow and transfer heat of Casson fluid in the extension of thermal conductivity, viscous dissipation, has been investigated close to the stagnation point flow. Chenna and Shankar [14] worked on Casson fluid flow is concerned with the impacts of heat source/sink on a non-linear stretching sheet. Medikare *et al.* [15] studied the Casson fluid stagnation point flow over a non-linear stretching sheet with viscous dissipation was examined for MHD. Jain [16] analyzed the Casson liquid flow evaluated past the Newtonian radiation in the presence of an exponentially acceleration infinite vertical plate.

*Corresponding author E-mail: nazimtufail@gmail.com

Ullah *et al*. [17] inspected the slip impact of Casson fluid non-linear stretchable plate on free convective MHD stream saturated by Newtonian heating in porous medium. Further, S. R. Mishra *et al.* [18] considered the effect of dissipation on MHD stagnation-point flow of Casson fluid through porous media over the stretching sheet. Furthermore, H. Sadaf and S.I. Abdelsalam [19] evaluated the hybrid nanofluid in a wavy non-uniform annulus with convective boundary conditions has adverse effects. K.B. Pavlov [20] examined the MHD flow of a flat surface deformation in an incompressible viscous fluid.

Scaling group transformations plays very important role to exploit the differential equations. Muhaimin et al. [21] analyzed scaling transformation for the impact of the fluid on velocity where fluid depends upon the temperature. Afify *et al*. [22] examined the slip flow impacts, two-dimensional magnetohydrodynamic (MHD) flows, Newtonian heating and thermal radiation flow over a permeable elastic sheet using the Lie symmetry. R. Kandasamy *et al*. [23] considered scaling transformation group on an MHD boundary layer through a porous extended surface for the impact of temperature-dependent nanofluid viscosity. Further, Md. Jashim Uddin *et al*. [24] probed a nanofluid slip flow across the convectively heated stretch sheet of heat generation for scaling group transformations of the MHD boundary layer. Furthermore, H. Dessie and N. Kishan [25] applied the scaling group on MHD thermal transfer impacts close to the stagnation point on linear strain sheets with varying viscosity and conductivity, viscous dissipation and heating source/sink effects.

A particular kind of Lie-group of transformations familiar as scaling in this study is utilized to detect the complete set of symmetries of the issue and then to examine which ones are suitable to providing group alternatives that are invariant or more particular similar. The technique decreases the non-linear partial differential equations which govern the movement of fluid into a strategy of combined ordinary differential equations. Due to some relationships between transformation parameters, the structure keeps invariant. With this transformation ordinary differential equations in third and second order are obtained that correspond to the momentum and energy equations. The fourth order Runge-Kutta method together with the shooting technique is used to solve these equations. The impacts of the Prandtl number, magnetic parameter, permeability parameter, velocity ratio, Eckert parameter, Casson fluid, viscosity parameter and heat source/sink parameter on velocity and temperature fields are examined and studied with the assistance of graphical representation and tabular forms.

2 Mathematical Formulations

Consider the two dimensional incompressible electrically conducting and steady MHD Casson fluid flow on a stretchable sheet through permeable media in the neighborhood stagnation point in the existence of variable viscosity, heat generation/absorption, variable thermal conductivity and viscous dissipation. The elastic sheet has invariable temperatureT_w, linear velocity $u_w(x)$. All exterior force fields excluding magnetic fields B_o are assumed to be zero. We have limited flow in the section y > 0 while stretchable sheet meets when plane y = 0. The axes x and y are respectively perpendicular along the sheet. Uniform magnetic field of strength $B_o$put out along the *y-axis*. The ambient medium differs from sheet temperature. The viscosity of the fluid will differ from temperature to constant assumptions of the other fluid characteristics. It can also be seen in Figure 1.

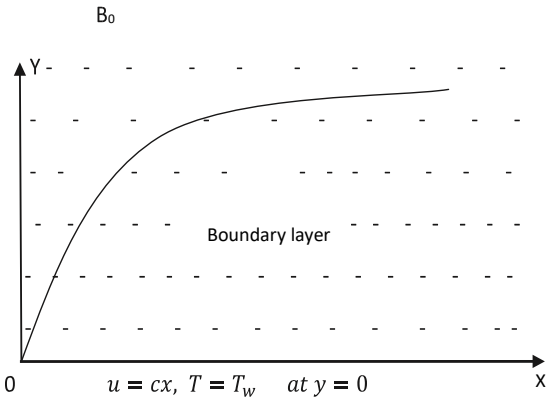

Fig. 1: Sketch of the physical problem.

By considering all assumptions, the governing equations of continuity, momentum and heat [26] will becomes

$$\frac{\partial u}{\partial x}+\frac{\partial v}{\partial y}=0, \tag{1}$$

$$u\frac{\partial u}{\partial x}+v\frac{\partial u}{\partial y}=-\frac{1}{\rho}\frac{\partial p}{\partial x}+\frac{1}{\rho}\left(1+\frac{1}{\beta}\right)\frac{\partial}{\partial y}\left(\mu\frac{\partial u}{\partial y}\right)-\frac{\sigma B_0^2}{\rho}u-\frac{\mu}{\rho k'}u, \tag{2}$$

$$u\frac{\partial T}{\partial x}+v\frac{\partial T}{\partial y}=\frac{1}{\rho c_p}\frac{\partial}{\partial y}\left(k^*\frac{\partial T}{\partial y}\right)+\left(1+\frac{1}{\beta}\right)\frac{\mu}{\rho c_p}\left(\frac{\partial u}{\partial y}\right)^2+\frac{Q_o}{\rho c_p}(T-T_\infty), \tag{3}$$

where u and v are velocity terms along the paths of x and y respectively, T is the temperature, T_∞ is the temperature far away from sheet, k^* is the thermal conductivity [27], Q_o is the volumetric heat generation $(Q_o > 0)$ or absorption $(Q_o < 0)$ coefficient, $c_p$is the specific heat, σ is the electric conductivity, p denotes the pressure along the $x-$axis, ρ is the fluid density (assumed constant), μ is the fluid viscosity, β is the non-Newtonian(Casson) fluid parameter and k' is the permeability of porous medium.

In the free stream $u = U(x) = bx$, the equation (2) reduces to

$$U\frac{dU}{dx} = -\frac{1}{\rho}\frac{\partial p}{\partial x} - \frac{\sigma B_0^2}{\rho}U - \frac{\mu}{\rho k'}U. \quad (4)$$

Eliminating $\frac{\partial p}{\partial x}$ from the equations (2) and (**Error! Reference source not found.**), we get

$$u\frac{\partial u}{\partial x} + v\frac{\partial u}{\partial y} = U\frac{dU}{dx} + \frac{1}{\rho}\left(1+\frac{1}{\beta}\right)\left[\frac{\partial \mu}{\partial T}\frac{\partial T}{\partial y}\frac{\partial u}{\partial y} + \mu\frac{\partial^2 u}{\partial y^2}\right] - \frac{\sigma B_0^2}{\rho}(u-U) - \frac{\mu}{\rho k'}(u-U). \quad (5)$$

The boundary conditions for the problem are given by

$$u = u\_w(x) = cx, v=0, \quad T=T\_w \text{ at } y=0,$$
$$u = U(x) = bx, T=T\_\infty \text{ as } y\longrightarrow\infty. \quad (6)$$

Here b and c>0 are stretching constants, T_wis the uniform wall temperature. Following Ling et al. [28] and Lai and Kulacki et al. [29], temperature-dependent viscosity of the form is taken as

$$\mu = \frac{\mu_\infty}{[1+a(T-T_\infty)]}, \quad (7)$$

$$\mu = \mu_\infty[1+a(T-T_\infty)]^{-1} = \mu_\infty[1-a(T-T_\infty)+a^2(T-T_\infty)^2 - \cdots], \cong \mu_\infty[1-a(T-T_\infty)], \quad (8)$$

where μ_∞ represents the constant of undisturbed viscosity and $a>0$ is a constant quantity. Note that the dimensionless temperature $\theta(x,y)$ can also be written as

$$\theta(x,y) = \frac{T(x,y)-T_r}{T_w-T_\infty} + \theta_r,\ \theta_r = \frac{T_r-T_\infty}{T_w-T_\infty},\ T_r = T_\infty - \frac{1}{a}. \quad (9)$$

Substituting (9) into (8), we immediately find

$$\mu = \mu_\infty[1-a(T_w-T_\infty)\theta]. \quad (10)$$

The deviation of1the thermal conductivity $k^*$is taken as

$$k^* = k_\infty(1+\varepsilon\theta).$$

The ε parameter that depends upon the nature of the fluid where k_∞ is thermal diffusivity at surface of temperature T_w.

2.1 Method of Solution

Introducing the stream functions and dimensionless temperature for the system i.e.,

$$u = \frac{\partial\psi}{\partial y}, \quad v = -\frac{\partial\psi}{\partial x}, \quad \theta = \frac{T-T_\infty}{T_w-T_\infty},$$

Where ψ denotes the stream1function.

Using the relations (8)-(10) in the boundary layer equations (**3**) and (**5**) we obtain the following equations

$$\frac{\partial\psi}{\partial y}\frac{\partial^2\psi}{\partial x\partial y} - \frac{\partial\psi}{\partial x}\frac{\partial^2\psi}{\partial y^2} = U\frac{dU}{dx} - A\nu_\infty\left(1+\frac{1}{\beta}\right)\frac{\partial\theta}{\partial y}\frac{\partial^2\psi}{\partial y^2} + \nu_\infty(1-A\theta)\left(1+\frac{1}{\beta}\right)\frac{\partial^3\psi}{\partial y^3} - \frac{\sigma B_0^2}{\rho_\infty}\left(\frac{\partial\psi}{\partial y}-U\right) - \frac{\nu_\infty}{k'}(1-A\theta)\left(\frac{\partial\psi}{\partial y}-U\right), \quad (11)$$

$$\frac{\partial\psi}{\partial y}\frac{\partial\theta}{\partial x} - \frac{\partial\psi}{\partial x}\frac{\partial\theta}{\partial y} = \frac{k_\infty\varepsilon}{\rho_\infty c_p}\left(\frac{\partial\theta}{\partial y}\right)^2 + \frac{k_\infty}{\rho_\infty c_p}(1+\varepsilon\theta)\frac{\partial^2\theta}{\partial y^2} + \frac{Q_o}{\rho_\infty c_p}\theta + \frac{\nu_\infty}{c_p(T_w-T_\infty)}(1-A\theta)\left(1+\frac{1}{\beta}\right)\left(\frac{\partial^2\psi}{\partial y^2}\right)^2. \quad (12)$$

Where $A = a(T_w-T_\infty), \nu_\infty = \frac{\mu_\infty}{\rho}$.

The boundary condition (**Error! Reference source not found.**) then becomes

$$\frac{\partial\psi}{\partial y} = cx,\ \frac{\partial\psi}{\partial x} = 0, \quad \theta = 1 \text{at } y=0,$$
$$\frac{\partial\psi}{\partial y} = U(x) = bx, \theta = 0 \text{as } y\longrightarrow\infty. \quad (13)$$

2.2 Scaling Group of Transformations.

Now present a simplified kind of Lie-group transformation that is scaling group transformation (Dessie *et al*. [28] and Mukhopadhyay *et al*. [29]),

$$\Gamma: x^* = xe^{\varepsilon\alpha_1},\ y^* = ye^{\varepsilon\alpha_2},\ \psi^* = \psi e^{\varepsilon\alpha_3},\ u^* = ue^{\varepsilon\alpha_4},\ v^* = ve^{\varepsilon\alpha_5},\ U^* = Ue^{\varepsilon\alpha_6},\ \theta^* = \theta e^{\varepsilon\alpha_7}. \quad (14)$$

Equation (**14**) may be considered as a point-transformation which transforms coordinates (x,y,ψ,u,v,θ) to the coordinates $(x^*,y^*,\psi^*,u^*,v^*,\theta^*)$. Substituting (**14**) in (**11**) and (**12**), we obtain,

$$e^{\varepsilon(\alpha_1+2\alpha_2-2\alpha_3)}\left(\frac{\partial\psi^*}{\partial y^*}\frac{\partial^2\psi^*}{\partial x^*\partial y^*} - \frac{\partial\psi^*}{\partial x^*}\frac{\partial^2\psi^*}{\partial y^{*2}}\right) = e^{\varepsilon(\alpha_1-2\alpha_6)}U^*\frac{dU^*}{dx^*} - e^{\varepsilon(3\alpha_2-\alpha_3-\alpha_7)}A\nu_\infty\left(1+\frac{1}{\beta}\right)\frac{\partial\theta^*}{\partial y^*}\frac{\partial^2\psi^*}{\partial y^{*2}} + e^{\varepsilon(3\alpha_2-\alpha_3)}\nu_\infty(1-A\theta^*e^{-\varepsilon\alpha_7})\left(1+\frac{1}{\beta}\right)\frac{\partial^3\psi^*}{\partial y^{*3}} - \frac{\sigma B_0^2}{\rho_\infty}\left(e^{\varepsilon(\alpha_2-\alpha_3)}\frac{\partial\psi^*}{\partial y^*} - U^*e^{-\varepsilon\alpha_6}\right) - \frac{\nu_\infty}{k'}(1-A\theta^*e^{-\varepsilon\alpha_7})\left(e^{\varepsilon(\alpha_2-\alpha_3)}\frac{\partial\psi^*}{\partial y^*} - U^*e^{-\varepsilon\alpha_6}\right), \quad (15)$$

$$e^{\varepsilon(\alpha_1+\alpha_2-\alpha_3-\alpha_7)}\left(\frac{\partial\psi^*}{\partial y^*}\frac{\partial\theta^*}{\partial x^*}-\frac{\partial\psi^*}{\partial x^*}\frac{\partial\theta^*}{\partial y^*}\right)$$
$$=\frac{k_\infty\varepsilon}{\rho_\infty c_p}e^{\varepsilon(2\alpha_2-2\alpha_7)}\left(\frac{\partial\theta^*}{\partial y^*}\right)^2$$
$$+\frac{k_\infty}{\rho_\infty c_p}e^{\varepsilon(2\alpha_2-\alpha_7)}(1+\varepsilon\theta^*e^{-\varepsilon\alpha_7})\frac{\partial^2\theta^*}{\partial y^{*2}}$$
$$+\frac{Q_o}{\rho_\infty c_p}\theta^*e^{-\varepsilon\alpha_7}+$$
$$\frac{\nu_\infty}{c_p(T_w-T_\infty)}e^{\varepsilon(4\alpha_2-2\alpha_3)}(1-A\theta^*e^{-\varepsilon\alpha_7})\left(1+\frac{1}{\beta}\right)\left(\frac{\partial^2\psi^*}{\partial y^{*2}}\right)^2. \quad (16)$$

Under the group of transformations Γ the system will remain invariant. We would like to have the following parameter relations, namely

$$\alpha_1+2\alpha_2-2\alpha_3=\alpha_1-2\alpha_6=3\alpha_2-\alpha_3-\alpha_7=3\alpha_2-\alpha_3$$
$$=\alpha_2-\alpha_3=-\alpha_6=\alpha_2-\alpha_3-\alpha_7,$$
$$\alpha_1+\alpha_2-\alpha3-\alpha_7=2\alpha_2-2\alpha_7=2\alpha_2-\alpha_7=-\alpha_7$$
$$=4\alpha_2-4\alpha_3=4\alpha_2-2\alpha_3-\alpha_7.$$

After fixing the parameters $\alpha_1=\alpha_3=\alpha_4=\alpha_6$ and $\alpha_2=\alpha_5=\alpha_7=0$. Thus, reduce into one parametric transformation:

$x^*=xe^{\varepsilon\alpha_1}$, $y^*=y$, $\psi^*=\psi e^{\varepsilon\alpha_1}$, $u^*=ue^{\varepsilon\alpha_1}$,

$v^*=v$, $U^*=Ue^{\varepsilon\alpha_1}$, $\theta^*=\theta$. (17)

We are expanding through Taylor's series

$$x^*-x=x\varepsilon\alpha_1,\quad y^*-y=0,$$
$$\psi^*-\psi=\psi\varepsilon\alpha_1,\quad u^*-u=u\varepsilon\alpha_1,$$
$$v^*-v=0,\quad U^*-U=U\varepsilon\alpha_1,\quad \theta^*-\theta=0. \quad (18)$$

The characteristic equations are

$$\frac{dx}{\alpha_1 x}=\frac{dy}{0}=\frac{d\psi}{\alpha_1\psi}=\frac{dU}{\alpha_1 U}=\frac{du}{\alpha_1 u}=\frac{dv}{0}=\frac{d\theta}{0}. \quad (19)$$

Thus, from equations (**19**) we obtain,

$$y=\eta,\quad \psi=xF(\eta),\quad \theta=\theta(\eta),$$

where F is an arbitrary function of η.

Using these transformation equations (**15**) and (**16**) becomes

$$\nu_\infty\left(1+\frac{1}{\beta}\right)(1-A\theta)F'''$$
$$-\left[F'^2-FF''-b^2+A\nu_\infty\left(1+\frac{1}{\beta}\right)\theta'F''\right]$$
$$-\left[\frac{\sigma B_o^2}{\rho_\infty}+\frac{\nu_\infty}{k'}(1-A\theta)\right](F'-b)=0, \quad (20)$$

$$\frac{k_\infty}{\rho_\infty c_p}(1+\varepsilon\theta)\theta''+\frac{k_\infty\varepsilon}{\rho_\infty c_p}\theta'^2+F\theta'+\frac{\nu_\infty x^2}{c_p(T_w-T_\infty)}(1-A\theta)\left(1+\frac{1}{\beta}\right)F''^2+\frac{Q_o}{\rho_\infty c_p}\theta=0. \quad (21)$$

The boundary conditions of equation (**13**) becomes

$$F'=c, F=0,\ \theta=1,\quad \text{at}\ \eta=0,$$
$$F'=b,\quad \theta=0\ \text{as}\ \eta\to\infty. \quad (22)$$

Introducing $\eta=v^\alpha c^\beta\eta^*, F=v^{\alpha'}c^{\beta'}F^*, \theta=v^{\alpha''}c^{\beta''}\bar\theta$ in equations (**20**) and (**21**) we get $\alpha'=\alpha=\frac{1}{2}$, $\alpha''=0, \beta=-1/2, \beta'=1/2, \beta''=0$. The equations (**20**) and (**21**) are transformed to

$$\left(1+\frac{1}{\beta}\right)(1-A\bar\theta)F^{*'''}-\left[F^{*'2}-F^*F^{*''}-\lambda^2+A\left(1+\frac{1}{\beta}\right)\bar\theta'F^{*''}\right]-[M+k_1(1-A\bar\theta)](F^{*'}-\lambda)=0, \quad (23)$$

$$(1+\varepsilon\bar\theta)\bar\theta''+\varepsilon\bar\theta'^2+Pr\,F^*\bar\theta'+\Pr Ec\,(1-A\theta)\left(1+\frac{1}{\beta}\right)F^{*''2}+S\,Pr\bar\theta=0, \quad (24)$$

where $Pr=\frac{u_\infty c_p}{k_\infty}$ is the Prandtl number, $S=\frac{Q_o}{c\rho c_p}$ present parameter of heat source/sink,parameter of velocity ratio is $\lambda=\frac{b}{c}$, $M=\frac{\sigma B_o^2}{\rho c}$ represent magnetic field, $Ec=\frac{c^2x^2}{c_p(T_w-T_\infty)}$is Eckert number, $k_1=\frac{\nu_\infty}{ck'}$ is the permeability parameter. Taking $F^*=f$and $\bar\theta=\theta$the equations (**23**) and (**24**) finally achieves the following form

$$\left(1+\frac{1}{\beta}\right)(1-A\theta)f'''-\left[f'^2-ff''-\lambda^2+A\left(1+\frac{1}{\beta}\right)\theta'f''\right]-[M+k_1(1-A\theta)](f'-\lambda)=0, \quad (25)$$

$$(1+\varepsilon\theta)\theta''+\varepsilon\theta'^2+Pr\left[f\theta'+Ec(1-A\theta)\left(1+\frac{1}{\beta}\right)f''^2+S\theta\right]=0. \quad (26)$$

The boundary conditions of Eq. (**22**) also reduces

$$f'=1,\quad f=0,\quad \theta=1\ \text{at}\ \eta=0,$$
$$f'=\lambda=\frac{b}{c},\quad \theta=0\ \text{as}\eta\to\infty. \quad (27)$$

Local Skin-friction. Local skin-friction1coefficient is represented as

$$C_{f_x}=\frac{\tau_w}{\rho(cv)^{\frac{1}{2}}}=x\left(1+\frac{1}{\beta}\right)f''(0)\quad \text{where}\quad \tau_w=\mu\left(\frac{\partial u}{\partial y}+\frac{\partial v}{\partial x}\right)_{y=0}.$$

Local Nusselt number. The rate of heat transfer according to the local Nusselt number is represented by

$$Nu_x=\left(\frac{\nu}{c}\right)^{\frac{1}{2}}\frac{q_w}{k^*(T_w-T_\infty)}=-\theta'(0)\quad \text{where}\quad q_w=-k^*\left(\frac{\partial T}{\partial y}\right)_{y=0}.$$

3 Result and Discussion

The set of non-linear boundary layer equations (**25**) - (**26**) with equations of boundary conditions (**27**) by applying Runge–Kutta fourth order strategy to find the numerically together with shooting system. Firstly, the higher order non-linear differential equations (**25**) - (**26**) are transformed into

differential equation of first order and furthermore, using the shooting method, they are converted into initial value problems. Once the issue has been bringing down to the initial value issue, so it is obtained due to Runge-Kutta fourth order strategy. The appropriate values for $f''(0)$ and$-\theta'(0)$ are selected and then integration is performed. Now this measurement the step size $\Delta(\eta)$ = 0.001 and the convergence criterion uses four decimal precision. The effects in the absence of suction / blowing in uniform viscosity are analyzed with the precision of the technique with H. Dessie *et al*. [30] and Mukhopadhyay *et al*. [31] as provided in Table Table1. The values of Local skin-friction coefficient $-(1+\frac{1}{\beta})f''(0)$ and temperature gradient $-\theta'(0)$ are mentioned in Table 2, Table 3 and Table 4 respectively. It is noted that from Table 2, as the velocity ratio parameter λ increase the local skin-friction coefficient $-\left(1+\frac{1}{\beta}\right)f''(0)$ decrease and temperature gradient $-\theta'(0)$ is increased. We can see it from the same table to rise variable viscosity A is increases the local skin-friction coefficient $-\left(1+\frac{1}{\beta}\right)f''(0)$ and decrease the temperature gradient $-\theta'(0)$. Now the permeability parameter k_1 enhance local skin-friction coefficient $-\left(1+\frac{1}{\beta}\right)f''(0)$ enhance but temperature gradient $-\theta'(0)$ is reduce. It is observed that in Table 3, as the Prandtl number Pr rise the local skin-friction coefficient $-\left(1+\frac{1}{\beta}\right)f''(0)$ and temperature gradient $-\theta'(0)$ is also raised. From the same table it can be notice that the local skin-friction coefficient $-\left(1+\frac{1}{\beta}\right)f''(0)$ and the temperature gradient $-\theta'(0)$ down with increase of heat source/sink parameter S. As the magnetic parameter M increases local skin-friction coefficient $-\left(1+\frac{1}{\beta}\right)f''(0)$ increases as well while the temperature gradient $-\theta'(0)$ decreases. It is predicted that in Table 4, as the Casson fluid β increase the local skin-friction coefficient $-\left(1+\frac{1}{\beta}\right)f''(0)$ increase but temperature gradient $-\theta'(0)$ is decrease. From the same table it can be noticed that the local skin-friction coefficient $-\left(1+\frac{1}{\beta}\right)f''(0)$ and the temperature gradient $-\theta'(0)$ up with down of Eckert number Ec. The effect of thermal conductivity parameter ε enhance local skin-friction coefficient $-\left(1+\frac{1}{\beta}\right)f''(0)$ and temperature gradient $-\theta'(0)$ are reduced.

Table1: The Skin-friction $-f''(0)$ and the wall temperature gradient $-\theta'(0)$ for two values of k_1 with $A=0$,
$S=0, \beta=\infty, Pr=1, \lambda=0, M=0, \varepsilon=0$ and $Ec=0$.

$-f''(0)$			
k_1	H. Dessie, N Kishan [30]	Mukhopadhyay [31]	Present study
1	1.414214	1.141213	1.414214
2	1.732051	1.732051	1.732050

$-\theta'(0)$		
H. Dessie, N Kishan [30]	Mukhopadhyay [31]	Present study
0.500008	0.500001	0.501258
0.447558	0.447553	0.447752

In Figures **2** to **10** for various flow parameters for example velocity ratio λ, thermal conductivity ε, magnetic parameter M, heat source/sink parameter S, Eckert number Ec, Prandt number Pr, variable viscosity parameter A, Casson fluid β and permeability parameter k_1 explained the graphically dimensionless velocity and temperature gradient.

It can be seen from **2** Figure **2(a)** that fluid velocity rises with rise of velocity ratio λ that, and the fluid temperature reduces because of enhance of velocity ratio λ which is plotted in Figure **2(b)**. Figures **3(a)** and **3(b)** show the impacts of thermal conductivity parameter ε on the velocity and temperature profiles respectively. Figure **3(a)** give away that the rise in the values of ε velocity profiles $f'(\eta)$ decreases. With rise the value of ε fluid temperature $\theta(\eta)$is also rise this results in a decrease in the heat transfer rate from the flow to the surface. Consequently, the coolant material with a tiny thermal conductivity parameter has a much quicker cooling rate. The influences on velocity and temperature profiles of the transverse magnetic field are displayed in Figures **4(a)** and **4(b)** respectively. From Figure **4(b)** it has been observed the rate of flow is greatly decreased with the enhance of M. It clearly shows that the transpose phenomena resist by transverse magnetic field. The velocity disappears everywhere at some stage huge distance from the sheet. The velocity reduces when the magnetic parameter M is increased. From the plots in Figure **4(b)**, it was noted to contribute to thickening of the thermal boundary layer by a transverse magnetic field. This can be seen from the reality, precisely the Lorentz force, which opposes the movement, that the applied transversal magnetic field produces the body strength. The flow resistance is accountable for the temperature increase. Figures **5(a)** and **5(b)** display the velocity and the temperature dispensation for different values of the heat generation parameter S. It is examined from Figure **5(a)** that the velocity profiles are substantially affected and decrease when the heat parameter value rises. It is clear from Figure **5(b)** the parameter heat generation value improves, as well as the temperature gradient along the boundary. Eckert number's impacts on dimensionless velocity and temperature are shown in Figures **6(a)** and **6(b)** respectively. The amount of Eckert is used to determine the ratio of fluid kinetic energy to the enthalpy differences of the boundary layer. It realizes transfer the kinetic energy into internal energy due to work done in the direction of viscous fluid stresses. If the plate is cooled, the Eckert number is positive i.e. that the plate loses heat to the fluid. More dissipative heat therefore leads temperature to increase but decreases in velocity. Figures also show that

the viscous dissipating impact is greater in temperature and less in velocity. For various terms of the

Table 2: Values of local skin-friction $-\left(\mathbf{1}+\frac{\mathbf{1}}{\boldsymbol{\beta}}\right)\boldsymbol{f''(0)}$ and wall gradient temperature $-\theta'(0)$ for different values of λ, A, k_1 for $Pr = 0.71, S = 0.1, M = 0.5,\ \beta = 0.6, Ec = 0.03, \varepsilon = 0.1$.

$\boldsymbol{\lambda}$	$\boldsymbol{A}$	$\boldsymbol{k_1}$	$-\left(\mathbf{1}+\frac{\mathbf{1}}{\boldsymbol{\beta}}\right)\boldsymbol{f''(0)}$	$\boldsymbol{-\theta'(0)}$
0.1	0.1	0.5	**0.8535**	**0.3788**
0.2	0.1	0.5	**0.7863**	**0.4118**
0.5	0.1	0.5	**0.5397**	**0.4892**
0.7	0.1	0.5	**0.3416**	**0.5315**
0.9	0.1	0.5	**0.1195**	**0.5686**
0.1	0.3	0.5	**0.9711**	**0.3650**
0.1	0.5	0.5	**1.1568**	**0.3436**
0.1	0.7	0.5	**1.5140**	**0.3101**
0.1	0.9	0.5	**2.7224**	**0.2405**
0.1	0.1	0.0	**0.7577**	**0.4095**
0.1	0.1	0.3	**0.8171**	**0.3979**
0.1	0.1	1.0	**0.9409**	**0.3751**
0.1	0.1	2.0	**1.0930**	**0.3497**
0.1	0.1	3.0	**1.2258**	**0.3296**

Table 3: Values of local skin-friction $-\left(\mathbf{1}+\frac{\mathbf{1}}{\boldsymbol{\beta}}\right)\boldsymbol{f''(0)}$and wall gradient temperature $-\theta'(0)$for differentvalues of Pr, S, M for $\lambda = 0.1,\ A = 1,\ k_1 = 0.5,\ \beta = 0.6, Ec = 0.03, \varepsilon = 0.1$.

$\boldsymbol{Pr}$	$\boldsymbol{S}$	$\boldsymbol{M}$	$-\left(\mathbf{1}+\frac{\mathbf{1}}{\boldsymbol{\beta}}\right)\boldsymbol{f''(0)}$	$\boldsymbol{-\theta'(0)}$
0.5	0.1	0.5	**1.8618**	**0.2655**
0.71	0.1	0.5	**1.8995**	**0.3105**
1.0	0.1	0.5	**1.9548**	**0.3795**
3.0	0.1	0.5	**2.2509**	**0.8035**
7.0	0.1	0.5	**2.5390**	**1.3476**
0.71	-0.3	0.5	**2.0658**	**0.5883**
0.71	-0.1	0.5	**1.9934**	**0.4637**
0.71	0.0	0.5	**1.9461**	**0.3869**
0.71	0.2	0.5	**1.7995**	**0.1675**
0.71	0.3	0.5	**1.6497**	**0.0345**
0.71	0.1	0.0	**1.6632**	**0.3348**
0.71	0.1	0.3	**1.8093**	**0.3194**
0.71	0.1	0.8	**2.0260**	**0.2990**
0.71	0.1	1.0	**2.1055**	**0.2922**

Table 4. Values of local skin-friction $-\left(\mathbf{1}+\frac{\mathbf{1}}{\boldsymbol{\beta}}\right)\boldsymbol{f''(0)}$ and wall gradient temperature $-\theta'(0)$ for different values of β, Ec, ε for $\lambda = 0.1,\ A = 0.1,\ k_1 = 0.5,\ Pr = 0.71,\ S = 0.1,\ M = 0.5$.

$\boldsymbol{\beta}$	$\boldsymbol{Ec}$	$\boldsymbol{\varepsilon}$	$-\left(\mathbf{1}+\frac{\mathbf{1}}{\boldsymbol{\beta}}\right)\boldsymbol{f''(0)}$	$\boldsymbol{-\theta'(0)}$
0.6	0.03	0.1	**0.8537**	**0.3833**
1.0	0.03	0.1	**0.9836**	**0.3618**
2.0	0.03	0.1	**1.1337**	**0.3393**
3.0	0.03	0.1	**1.2016**	**0.3299**
5.0	0.03	0.1	**1.2659**	**0.3215**
0.6	0.0	0.1	**0.8539**	**0.3992**
0.6	0.3	0.1	**0.8520**	**0.2401**
0.6	0.5	0.1	**0.8508**	**0.1345**
0.6	0.7	0.1	**0.8496**	**0.0292**
0.6	0.03	0.0	**0.8543**	**0.4124**
0.6	0.03	0.3	**0.8528**	**0.3873**
0.6	0.03	0.5	**0.8520**	**0.3026**
0.6	0.03	3.0	**0.8477**	**0.1495**
0.6	0.03	5.0	**0.8467**	**0.1204**

Prandt number Pr, the velocity and the temperature profiles are shown in Figures **7(a)** and **7(b)** respectively. The Prandtl1number explain the ratio of momentum diffusivity to the thermal diffusivity. From Figure **7(a),** it is visible that an enhance in the Prandt number than velocity profile also rises. From Figure **7(b)**, the increase in the Prandt number is shown to reduce the thermal boundary layer thickness and generally a reduced boundary layer average temperature. The reason is because lower Pr values equate to higher thermal conductivity and thus for greater Pr values, heat can spread faster away from the heated surface. This is why the boundary layer is thicker and heat transmission velocity is lowered for lower Prandt numbers. Impacts of viscosity parameter A on the velocity and temperature profiles are clearly displayed in Figures **8(a)** and **8(b)** respectively. Fluid velocity reduces with enhancing values of viscosity parameter is observed that form the Figure **8(a)**. It can be seen from Figure **8(b)** that the temperature profiles up with enhance of variable viscosity. That's because the skin friction coefficient is rise by rising the variable viscosity parameter which decreases the velocity of the fluid. Physically, when friction increases, thermal viscosity enhances the area1of the stretchable surface in contact with the flow rise, hence the friction on the surface is pass to the flow generated by the heat. This results in the temperature of the surface is rise and the flow is heated. From Fig. **9** are drawn to the velocity profile $f'(\eta)$and temperature profiles $\theta(\eta)$ respectively, for various term of permeability parameter k_1. The impact of k_1 contributes to a reduction in velocity profile $f'(\eta)$ for uniform and variable viscosity. From the Fig.**9(b)** the temperature profiles can be seen up with a permeability parameter k_1 rise in both instances of variable and uniform viscosity. From Fig. **10** are drawn to the velocity profile $f'(\eta)$and temperature profiles $\theta(\eta)$ for various values of Casson fluid parameter β. In Fig. **10(a)** the effect of β leads to down the velocity profile $f'(\eta)$ in instance of increasing in variable viscosity. From1the Fig. **10(b)** it can be observed that the temperature profiles increase with increment in Casson fluid parameter β, in both instances of variable and uniform viscosity.

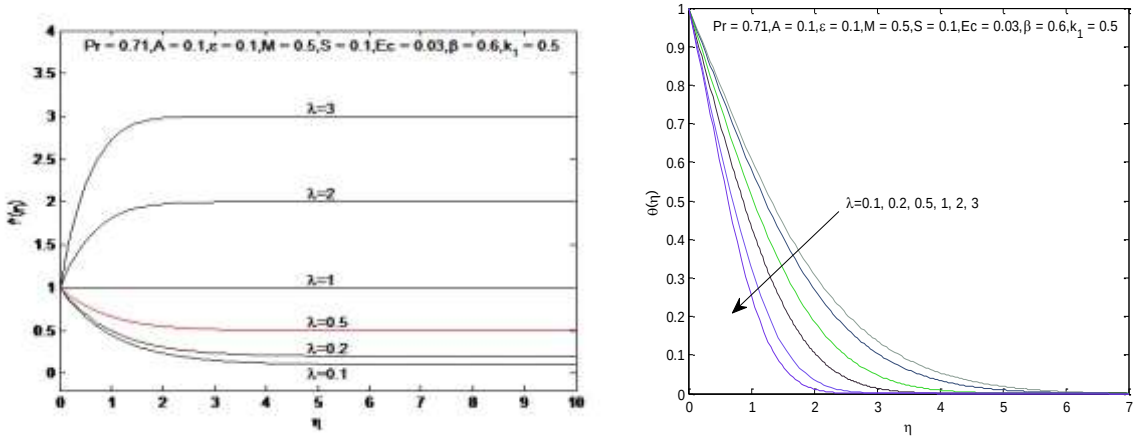

2(a) **2(b)**

Fig. 2: $f'(\eta)$and **$\theta(\eta)$** profiles for various values of λ.

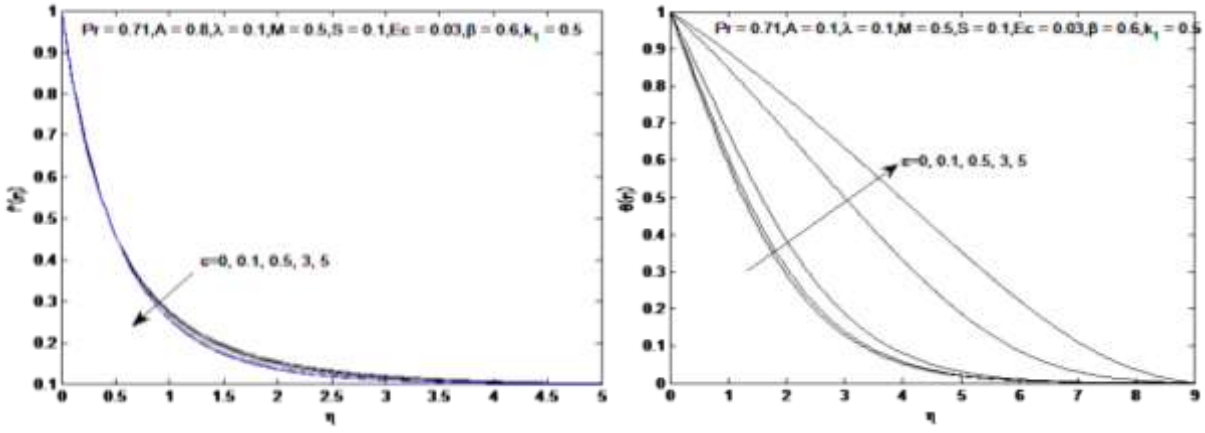

3(a) 3(b)

Fig.3: $f'(\eta)$and **$\theta(\eta)$** profiles for various values of ε.

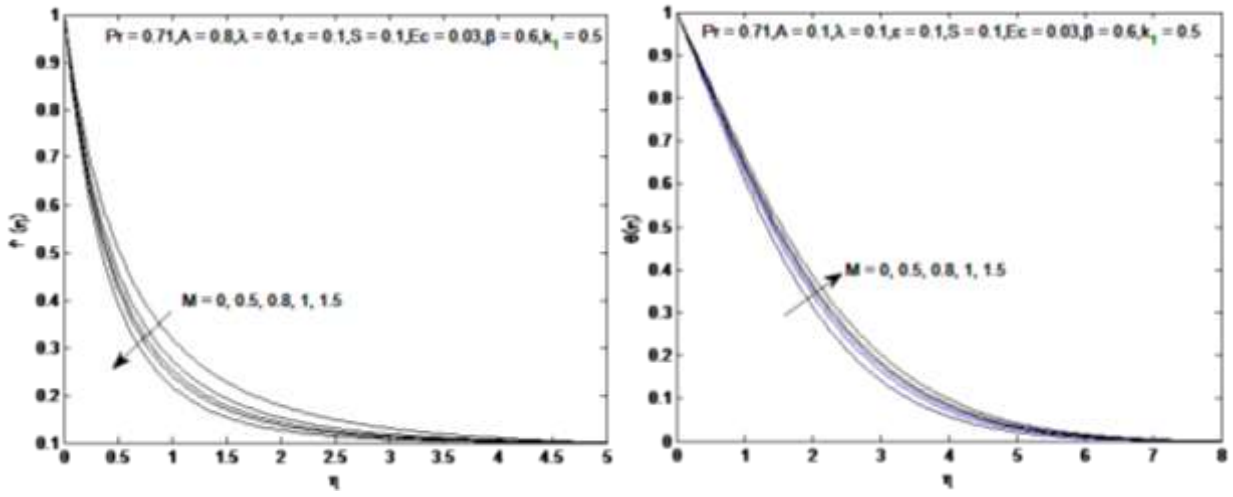

4(a) 4(b)

Fig. 4: $f'(\eta)$and $\theta(\eta)$ profiles for various values of M.

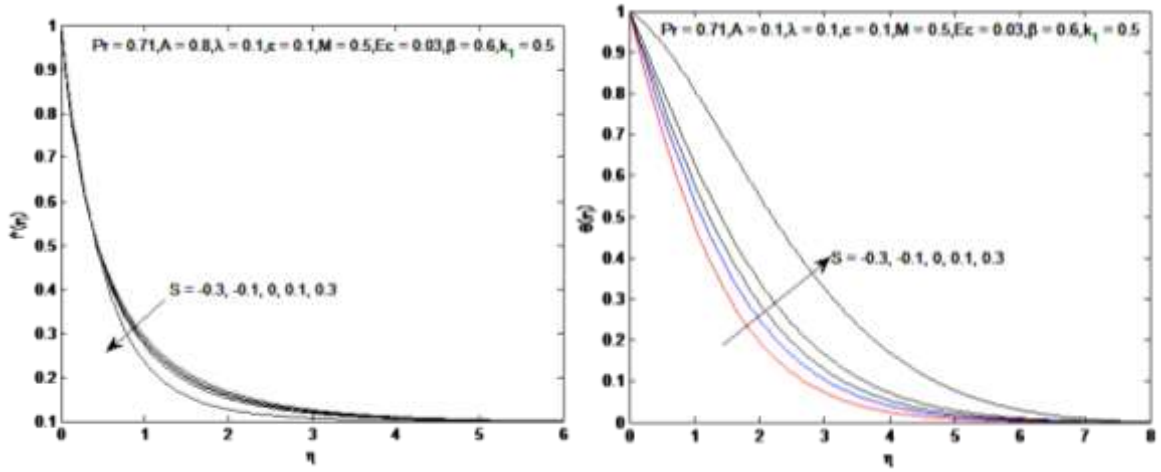

5(a) 5(b)

Fig. 5: $f'(\eta)$and $\theta(\eta)$ profiles for various values of S.

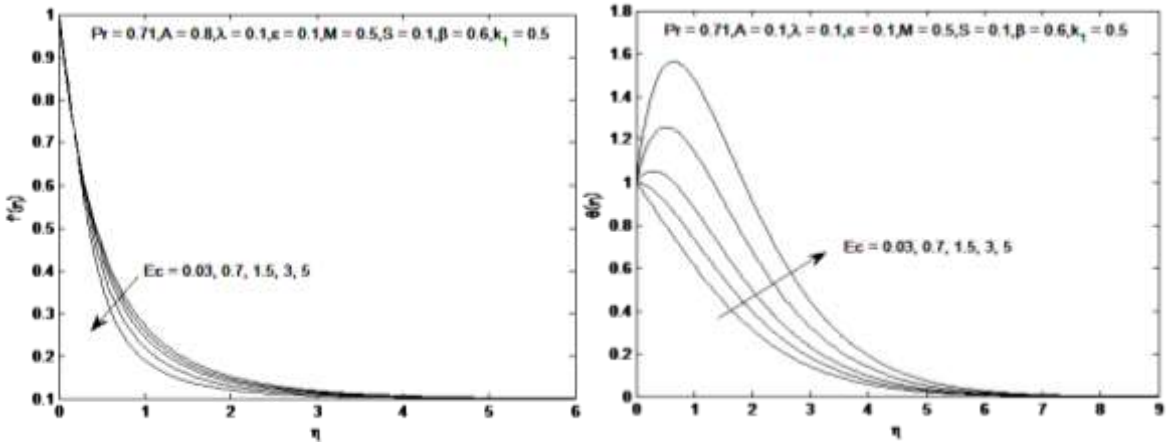

6(a) 6(b)

Fig.6: $f'(\eta)$ and $\theta(\eta)$ profiles for various values ofEc.

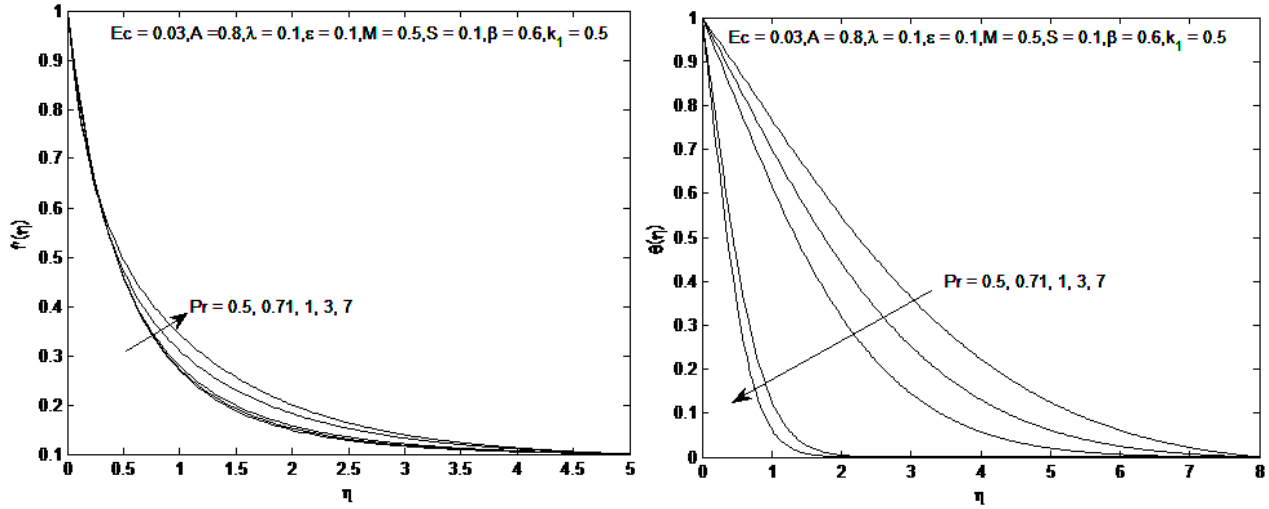

7(a) 7(b)

Fig. 7: $f'(\eta)$and $\theta(\eta)$ profiles for various values ofPr.

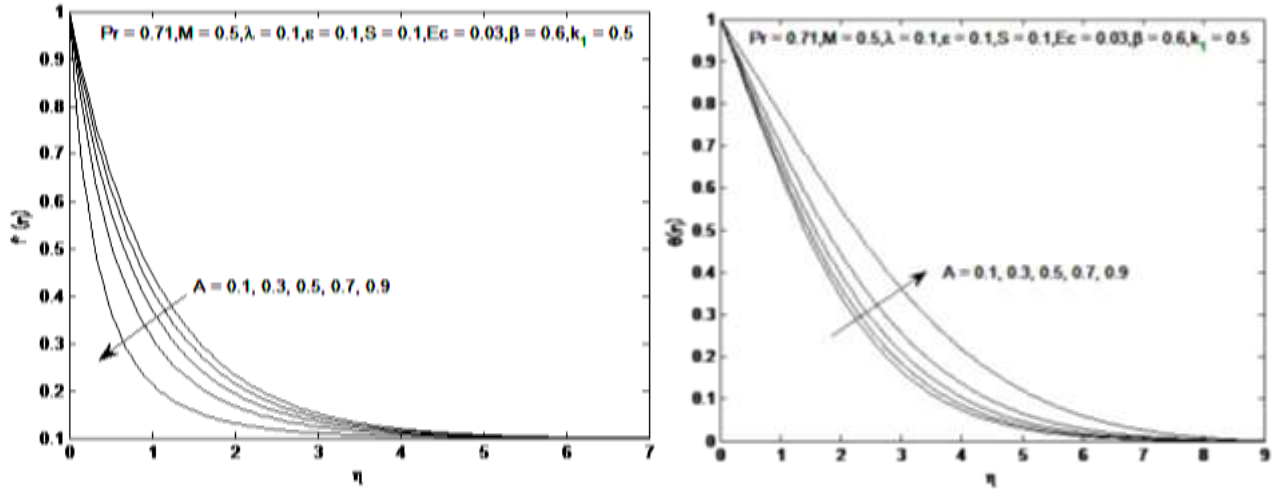

8(a) 8(b)

Fig. 8: $f'(\eta)$and $\theta(\eta)$ profiles for various values of A.

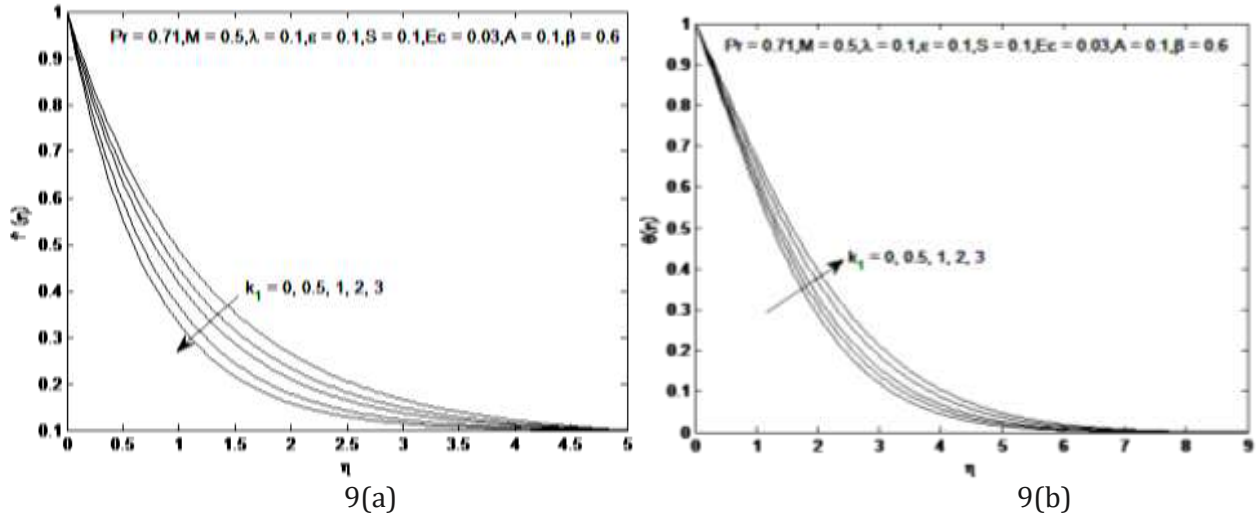

9(a) 9(b)

Fig. 9: $f'(\eta)$and $\theta(\eta)$ profiles for various values of k_1.

magnetic field M, Eackert number Ec,

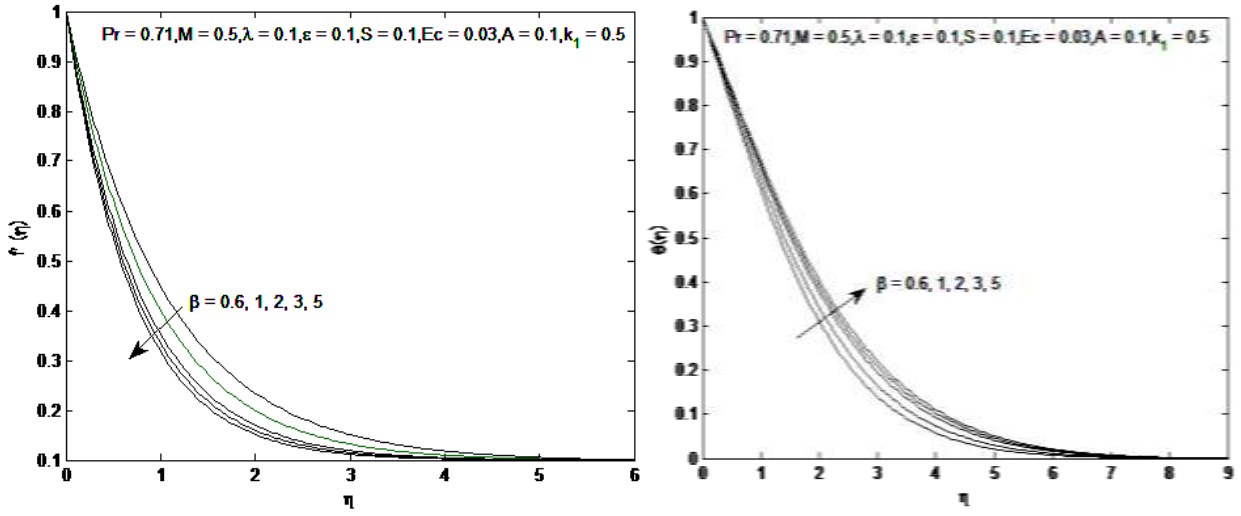

10(a) 10(b)

Fig.10: $f'(\eta)$and $\theta(\eta)$ profiles for various values of β.

Conclusion

In this work, we have studied that the variable viscosity and thermal conductivity of MHD Casson fluid flow through a linearly stretchable sheet implanted in porous media with viscous dissipation and heat source/sink impacts. The velocity of stretching and surface temperature shall differ linearly with the range from the point of stagnation. The governing equations were altered to dimensionless partial differentialequations intoordinary differential equ ations due to the help of scaling group of transformations. To fix the governing equations of motion, the powerful technique of lie group is used. This method helps eliminate the problems encountered by the non-linear characteristic of the partial differential equations when solving equations. In order to understand the mathematical model, the scaling symmetry group is a most important method. By apply the Runge Kutta fourth order with shooting techniques; transformed governing equations have been numerically solved in the current work. For a number of specific cases from this work, numerical outcomes are very well in agreement with earlier published data. The following results can be taken from this work:

- The velocity of fluid f' rise when velocity ratio parameter λ is rise and Prandtl number Pr whereas it decreases with the increase in thermal conductivity parameter ε, magnetic field M, Eackert number Ec, Casson fluid β, viscosity parameter A and permeability of porous medium k_1.
- The temperature profile θ increases with increased thermal conductivity parameter ε, β, viscosity parameter A and permeability of porous medium k_1, whereas the temperature of fluid decreases with increased Prandtl number Pr and velocity ratio parameter λ.
- The skin friction coefficient $-\left(1+\frac{1}{\beta}\right)f''(0)$increase with rising the value of permeability constant k_1, viscosity parameter A, magnetic field parameter M, Casson fluid parameter β and Prandtl number Pr whereas its value decrease with increase the Eckert number Ec, thermal conductivity parameter ε, velocity ratio parameter λ and source/sink parameter S.
- The local Nusselt number $-\theta'(0)$ increases with the increased effect of velocity ratio parameter λ and Prandtl number Pr while rise the magnetic field parameter M, viscosity parameter A, permeability constant k_1, Casson fluid parameter β, Eckert number Ec, thermal conductivity parameter ε and source/sink parameter S causes the local Nusselt number to decrease.

References

[1] L. J. Crane, Flow past a stretching plate, Z. Angew. Math. Phys., **21**, 645–647(1970).

[2] C.K. Chen, M. I. Char, Heat transfer of a continuous stretching surface with suction or blowing. J. Math. Anal. Appl., **135**, 568–580 (1988).

[3] I. Pop, T.Y. Na, Unsteady flow past a stretching sheet. Mech. Res. Commun., **23**, 413–422 (1996).

[4] K. Vajravelu, Viscous flow over a nonlinearly stretching sheet. Appl. Math. Comput., **124**, 281–288 (2001).

[5] R. Cortell, Viscous flow and heat transfer over a nonlinearly stretching sheet, Appl. Math. Comput., **184**, 864–873(2007).

[6] L. Zheng, L. Wang, X. Zhang, Analytic solutions of unsteady boundary flow and heat transfer on a permeable stretching sheet with non-uniform heat source/sink, Commun. Nonlinear Sci. Numer. Simulat., **16**, 731–740 (2011).

[7] K. Bhattacharyya, Effects of radiation and heat source/sink on unsteady MHD boundary layer flow and heat transfer over a shrinking sheet with suction/injection, Front. Chem. Sci. Eng., **5**, 376–384 (2011).

[8] M.A.A. Mahmoud, S. E. Waheed, MHD flow and heat transfer of a micro polar fluid over a stretching surface with heat generation (absorption) and slip velocity, J. Egypt. Math. Soc, doi.org/10.1016/j.joems.2011.12.009 (2012).

[9] N. A. Casson FlowEquation for the Pigment Oil Suspensions of the Printing Ink Type, New York: Pergamon (1959).

[10] R. K. Dash, K. N. Mehta and G. Jayaraman, Casson fluid flow in a pipe filled with a Homogeneous porous medium, International Journal Engineering Science., **34**, 1145 (1996).

[11] Y. C. Fung Biodynamics Circulation (New York: Springer-Verlag)(1984).

[12] H. M. Shawky, Magnetohydrodynamic Casson fluid flow with heat and mass transfer through a porous medium over a stretching sheet, Journal of Porous Media., 15(2012).

[13] S. Shateyi and G. T. Marewo Proceedings of the 7th International Conference on Finite Differences, Finite Elements, Finite Volumes, Boundary Elements (Gdansk, Poland)., (2014).

[14] C. Sumalatha and S. Bandari,Effects of Radiations and Heat Source/Sink on a Casson Fluid Flow over Nonlinear Stretching Sheet, World Journal of Mechanics., **5**, 257, (2015).

[15] M. Medikare, S. Joga and K. Chidem, MHD Stagnation Point Flow of a Casson Fluid over a Nonlinearly Stretching Sheet with Viscous Dissipation, American Journal of Computational Mathematics., **6**, 37 (2016).

[16] P. Jain International, Casson fluid past an exponentially accelerated surface with Newtonian heating in the presence of thermal radiation, Journal of Engineering Research and General Science., **3**, 873 (2015).

[17] I. Ullah, S. Shafie and I. Khan, Effects of slip condition and Newtonian heating on MHD flow of Casson fluid over a nonlinearly stretching sheet saturated in a porous medium, Journal of King Saud University-Science., (2016).

[18] S. R. Mishra, A. Ara and N. A. Khan, Dissipation Effect on MHD Stagnation-Point Flow of Casson Fluid Over Stretching Sheet Through Porous Media, Mathematical Sciences Letters., **7(1)**, 13-20 (2018).

[19] H. Sadaf and S.I. Abdelsalam, Adverse effects of a hybrid nanofluid in a wavy non-uniform annulus with convective boundary conditions, Royal Society of Chemistry., **10**, 15035-15043 (2020).

[20] K.B. Pavlov, Magneto hydrodynamic flow of an incompressible viscous fluid caused by the deformation of a plane surface, Magn. Gidrod., **10**, 146–148(1974).

[21] Muhaimin, R. Kandasamy, I. Hashim, Scaling transformation for the effects of chemical reaction on free convective heat and mass transfer in the presence of variable stream conditions, Chem. Eng. Res. Des., **88(10)**, 1320-1328, (2010).

[22] A. A. Afify, M. J. Uddin, M. Ferdows, Scaling group transformation for MHD boundary layer flowover permeable stretching sheet in presence of slip flow with Newtonian heating effects, applied mathematics (eng. ed) DOI10.1007/s10483-014-1873-7.,**35(11)**,1375–1386(2014).

[23] R. Kandasamy, I. Muhaimin, G. Kamachi, Scaling group transformation for the effect of temperature-dependent Nanofluid viscosity on an MHD boundary layer past a porous stretching surface, Journal of Applied Mechanics and Technical Physics., **52(6)**, 931–940 (2011).

[24] Md. Jashim Uddin, W. A. Khan, A. I. Md. Ismail, Scaling Group Transformation for MHD Boundary Layer Slip Flow of a Nanofluid over a Convectively Heated Stretching Sheet with Heat Generation, Mathematical Problems in Engineering Volume, Article ID 934964, 20 pages (2012).

[25] H. Dessie and N. Kishan, Scaling group analysis on MHD effects on heat transfer near stagnation point on a linearly stretching sheet with variable viscosity and thermal conductivity, viscous dissipation and heat source/sink. TAM., **42(2)**, 111-133(2015).

[26] W.M. Kays and M.E. Crawford, Convective heat and mass transfer, 4th ed. McGraw Hill, New York., (2005).

[27] M.A. Seddeek and A.M. Salem, Laminar mixed convection adjacent to vertical continuously stretching sheet with variable viscosity and variable thermal diffusivity. Heat Mass Transfer., **41**, 1048–1055(2005).

[28] J.X. Ling, A. Dybbs, Forced Convection over a flat plate submersed in a porous media: variable viscosity case, ASME Winter Annual Meeting, Boston., 13–18(1987).

[29] F.C. Lai, F.A. Kulacki, The effect of variable viscosity on convective heat transfer along a vertical surface in a saturated porous medium, Int. J. Heat Mass Transfer., **33**, 1028–1033, (1999).

[30] H. Dessie and N. Kishan, MHD effects on heat transfer over stretching sheet embedded in porous medium with variable viscosity, viscous dissipation and heat source/sink. ASEJ., **5(3)**, 967-977 (2014).

[31] S. Mukhopadhyay, G.C. Layek, S.A. Samad, Study of MHD boundary layer flow over a heated stretching sheet with variable viscosity, Int. J. Heat Mass Transfer., **48**, 4460–4466 (2005).